Ion pairing in radical cations: the example of 9,9′-bianthryl

Md. Nadeem Khan, Cornelia Palivan, Frédérique Barbosa, Jérôme Amaudrut and Georg Gescheidt*

Institute of Physical Chemistry, Department of Chemistry, University Basel, Klingelbergstrasse 80, CH-4056 Basel, Switzerland

Received (in Cambridge, UK) 20th April 2001, Accepted 18th July 2001
First published as an Advance Article on the web 9th August 2001

9,9′-Bianthryl (**1**) was one-electron oxidized under several different conditions. Depending on the counter anion and the solvent, two structures of the corresponding radical cation were established. The temperature behaviour of the EPR spectra is interpreted in terms of a loose ion pair formed preferentially at low temperatures with the spin and the charge delocalised within the entire π system of $\mathbf{1}^{\bullet+}$. At increased temperatures and with CF_3COO^- as the counterion and trifluoroacetic acid or 1,1,1,3,3,3-hexafluoropropanol as the solvent, a tight ion pair is formed which resembles the anthracene radical cation. The distinction between the two species can also be drawn from the optical spectra. Quantum mechanical calculations indicate that the formation of the radical cation is guided with a change of the twist angle between the two anthracene planes from 90° to *ca.* 74°.

Introduction

Ion pairing significantly contributes to the persistence of charged radicals and also influences their structure in terms of symmetry, conformational mobility and/or electron and charge delocalisation. Many classical examples can be found in the literature.[1] However most of these studies are limited to the interactions of radical anions with (alkali) metal counter cations produced by the reaction of the parent molecule with elemental metal.[2–5] Analogous methods leading to radical cations with well established counterions do not exist and the knowledge about the radical cation–counter anion interactions is lacking.

The variety of methods to generate radical cations ranges from oxidation with sulfuric acid, over reaction with Lewis acids ($AlCl_3$, $SbCl_5$. . .),[6] metal salts ($Tl(OCOCCF_3)_3$, $Hg(OCOCCF_3)_2$, $AgClO_4$. . .),[7] organic agents (tris(*p*-bromophenyl)ammonium hexachloroantimonate, DDQ, chloranil. . .),[8,9] zeolites,[10–12] to high-energy irradiation in freon matrices.[13] Whereas the structure of the thus obtained radical cations has been established by spectroscopic methods, in particular EPR, the character and the influence of the (counter) anions produced in the electron-transfer reaction are still equivocal.

In this contribution we try to shed some light on the interconversion between tight and loose ion pairs. We will report on the radical cations generated from 9,9′-bianthryl (**1**) under several different conditions and discuss the charge and spin delocalisation in terms of counterion–solvent combinations and the temperature dependence of the EPR spectra.

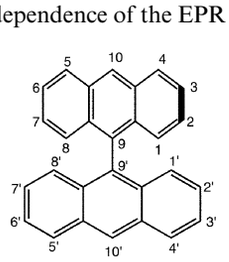

1

Experimental

9,9′-Bianthryl (**1**) was prepared by the reported procedure.[14] All solvents used were of highest available quality from Merck: CH_2Cl_2 (dried over molecular sieves under vacuum), trifluoroacetic acid (TFA) and 1,1,1,3,3,3-hexafluoropropan-2-ol (HFP) were used as purchased. The oxidation reactions were performed by mixing the solutions of oxidant and the parent compounds (~10^{-3} M) under high vacuum (~10^{-5} Torr) at temperatures just above the freezing points of the reaction solutions. Usually 1 : 1, 1 : 2 and 2 : 1 molar ratios of substrate : oxidant were used. The electron acceptors employed were thallium(III) trifluoroacetate (TTFA), tris(*p*-bromophenyl)-ammonium hexachloroantimonate, 2,3-dichloro-5,6-dicyano-benzoquinone (DDQ) and $AlCl_3$. In the case of oxidation with DDQ, traces of TFA were introduced to protonate the anionic species and thus avoid very rapid nucleophilic/electron transfer follow-up reactions of the resulting radical cation.[9]

Electronic absorption spectra were recorded inside the microwave cavity in the same region of the sample tube and simultaneously with the EPR spectra using a specially developed coupling of fibre optics to the cavity of the EPR spectrometer (simultaneous EPR–optical spectroscopy, SEOS)[15] and a TIDAS diode-array spectrometer (220–1021 nm, J & M, Aalen, Germany). EPR spectra were recorded on a Varian E 9 spectrometer while Bruker ESP 300 served for ENDOR measurements. Both spectrometers were fitted with variable temperature units and the spectra were recorded at *ca.* 10 K intervals between the freezing point of the reaction mixture and room temperature. Spectral simulations were performed by the public domain program Winsim.[16]

Quantum-mechanical calculations were performed with the Gaussian 94 package.[17] Geometry optimizations and the determination of the Fermi contacts (hfcs) were performed at the UB3LYP/6-31G*[18,19] level of theory.

Results

Oxidation of 9.9′-bianthryl (**1**) was marked by the appearance of a green colour in the reaction solutions. Treatment with TTFA in CH_2Cl_2 at 193 K yielded the spectra shown in Fig. 1. The ENDOR spectrum revealed three hfcs of 0.153 (8 H), 0.066 (8 H) and 0.378 (2 H) mT (type ***A***, resembling the data in ref. 20, Table 1) and the thus simulated spectra showed a favourable agreement with the experimental ones. The electronic spectra recorded simultaneously with EPR are represented in Fig. 1. However, as the temperature was gradually raised, another well-defined spectrum appeared at 263 K (type ***B***, *cf.* Fig. 2).

 DOI: 10.1039/b103559m

The ENDOR technique (Fig. 2) and simulation of the EPR exhibited hfcs with doubled values but halved multiplicities (Tables 1 and 2) compared to the low-temperature spectra. Alternative concentration ratios of the reactants (see Experimental) yielded similar results. Oxidation with $AlCl_3$ and tris-(*p*-bromophenyl)ammonium hexachloroantimonate in CH_2Cl_2 gave only broad poorly resolved signals, which could not be assigned unambiguously. Reaction with TTFA in HFP led to spectra of type ***B*** (no temperature and concentration dependence). The electronic spectrum taken under the latter conditions is included in Fig. 2. Oxidation in TTFA–TFA showed intense and well characterised spectra of type ***B*** (no concentration and temperature dependence). Oxidation by DDQ in TFA and HFP initially showed spectra characteristic of type ***A*** at 263 K, but at 283 K were converted to type ***B***. Rapid re-cooling of the sample yielded type ***A*** spectra. The results are compiled in Table 1.

The transition between the EPR spectra of type ***A*** to ***B*** is shown in Fig. 3. The simulations of the experimental signals could be accomplished by the superposition of the two species ***A*** and ***B*** whereas the use of a two-jump model did not yield matching results.

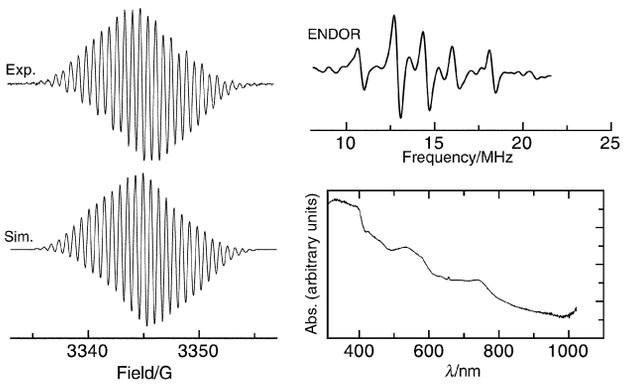

Fig. 1 EPR (experimental and simulated) ENDOR and optical spectra (type ***A***) obtained after TTFA oxidation of **1** in CH_2Cl_2, T = 193 K.

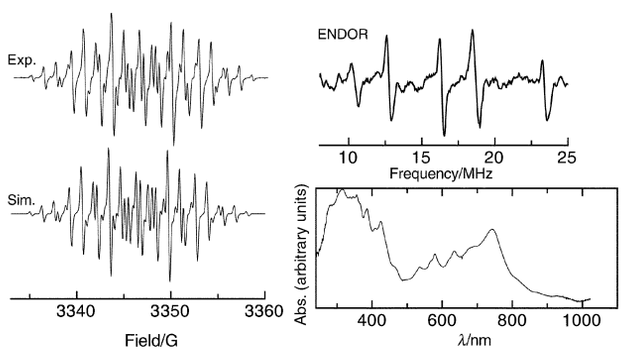

Fig. 2 EPR (experimental and simulated) ENDOR and optical spectra (type ***B***) obtained after TTFA oxidation of **1** in TFA, T = 263 K.

Table 1 Experimental conditions and EPR-spectral types

Radical	Oxidant	Solvent	EPR Type	
$\mathbf{1}^{\bullet+}$	TTFA	CH_2Cl_2	***A*** (193–223 K)	***B*** (243–283 K)
	TTFA	HFP		***B***
	TTFA	TFA		***B***
	DDQ	CH_2Cl_2	***A*** (193–243 K)	***B*** (263–283 K)
	DDQ	HFP	***A*** [a]	***B***
	DDQ	TFA	***A*** [a]	***B***
	$SbCl_5$	CH_2Cl_2	***A*** [b]	

[a] At 263 K, the solvent starts to freeze. Below 273 K the spectrum of type ***A*** starts to grow in. [b] Taken from ref. 20.

Discussion

Localisation–delocalisation

One electron oxidation of aromatic compounds leads primarily to the corresponding radical cations which often exist in monomeric or dimeric form (intervalence compounds).[21–25] Both types of ions have been characterised by EPR, and as a rule of thumb, the hyperfine splitting constants of a dimer are supposed to be half of those of the monomer radical cation with doubled multiplicities.[26]

An analogous relation holds if the molecule is composed of two identical moieties and the spin and the charge either get localised on one half of the molecule or are entirely delocalised. The EPR data representing the spectra of type ***B*** closely resemble those found for the (monomeric) radical cation of anthracene (Table 2) with the missing hfc at the 9 position, thus providing a straightforward assignment of all hfcs. On the other hand, the halved hfcs and doubled multiplicities characteristic for the type ***A*** spectra (Table 1) could either mirror a dimer (Fig. 4) or a system in which the spin and the charge are delocalised within the entire π system of $\mathbf{1}^{\bullet+}$. An answer as to which of these two delocalised is observed can be given by studying the temperature behaviour of the EPR spectra.

Temperature dependence

The conditions under which the charge of the monocations is localised in one electrophoric subunit or undergoes a rapid hopping between the subunits, leading to an effective delocalisation within the time scale of the EPR experiment, are indicative to distinguish between ion pairing or dimer formation. It was shown that oxidation of anthracene leads to monomeric radical cations but also a cyclophane-like face-to-face (sandwich) dimer ($[anthracene]_2^{\bullet+}$).[27] The formation of delocalised $[\pi\text{–}\pi]^{\bullet+}$ dimers is induced at high concentration of the parent π system and high temperatures. In contrast, in radical ions composed of two or more identical aromatic units, tight ion pairing impedes the delocalisation of the unpaired electron at increased temperatures due to the decrease of the relative permittivity of the solvent.[1,20]

Both phenomena (Fig. 4) have to be taken into account for the analysis of the EPR spectra obtained after oxidation of **1**.

Generally, the EPR spectra representing a structure in which the spin is confined to one molecular moiety (type ***B***) are detected at high temperatures whereas the hfcs characteristic

Table 2 EPR parameters for radical cations $\mathbf{1}^{\bullet+}$ according to spectral types ***A*** and ***B***. The ^1H hfcs are given in mT. The reference data of $[anthracene]^{\bullet+}$ and $[anthracene]_2^{\bullet+}$ are taken from ref. 27 and references cited therein

	H(1,4,5,8)	H(1′,4′5′,8′)	H(2,3,6,7)	H(2′,3′,6′,7′)	H(10)	H(10′)	*g* factor
A (exp.) [a]	−0.138	−0.138	−0.059	−0.059	−0.353	−0.353	2.00333
A (calc.) [b]	−0.153	−0.153	−0.053	−0.053	−0.397	−0.397	
B (exp.) [a]	−0.297	—	−0.130	—	−0.639	—	2.00291
$[Anthracene]_2^+$	−0.308		−0.138		−0.647 (9,10)		
$[Anthracene]_2^+$	0.142	0.142	0.071	0.071	0.325	0.325	

[a] Values vary by *ca.* 5% depending upon oxidant/solvent combination. [b] UB3LYP/6-31G*.

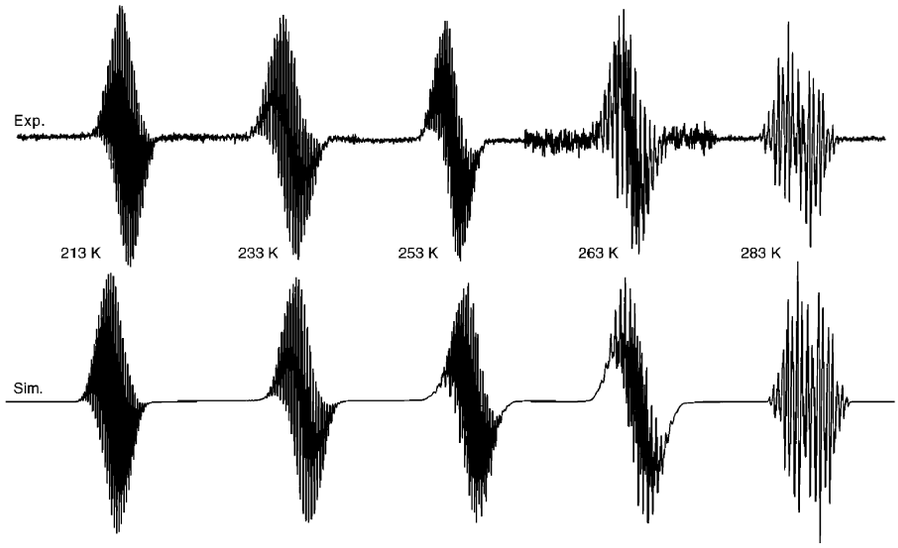

Fig. 3 EPR spectra of $\mathbf{1}^{\bullet+}$, counterion CF_3COO^-; solvent CH_2Cl_2 depending on temperature and the corresponding simulations.

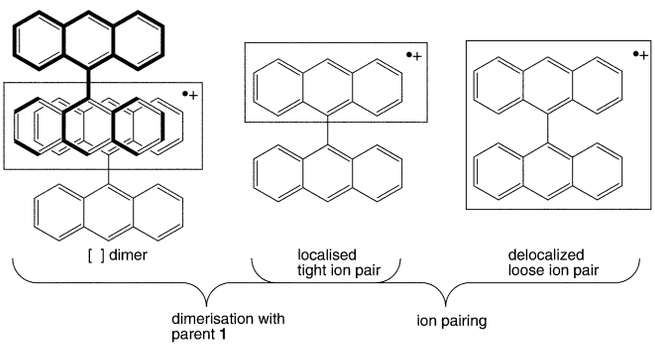

Fig. 4 π Dimers and localisation–delocalisation of spin and charge in 9,9′-bianthryl (counterions not shown).

for a delocalised species are found in the low-temperature domain (Table 1). Moreover, an excess of parent **1** does not lead to a drastic change of the EPR pattern. This is characteristic for ion pairing being responsible for the localisation–delocalisation phenomenon observed and resembles the results obtained with the radical anions of **1**.[28]

Counterions—the grey zone

The localised form of $\mathbf{1}^{\bullet+}$ (EPR type ***B***) is present when the oxidation reactions are performed with TTFA or TFA as the (co)solvent, *i.e.*, CF_3COO^- has to be considered as the counterion. The tight binding between this anion and $\mathbf{1}^{\bullet+}$ is exhibited by the appearance of the type ***B*** EPR spectra. There is no line broadening or additional splitting visible which could be directly attributed to the interaction with CF_3COO. Although ^{19}F is a very sensitive nucleus where an s-orbital spin population of only 0.005% at the F atom already leads to a ^{19}F hfc of 0.05 mT (readily detectable by EPR), the F atoms are presumably too remote from the radical cation to carry a detectable amount of spin.

The delocalised (EPR type ***A***) radical cation of **1** can be observed after oxidation with TTFA and DDQ in CH_2Cl_2, at low temperatures and with DDQ in HFP as well as $SbCl_6$ in CH_2Cl_2. After reaction with DDQ with TFA added and with TTFA the electron transfer reaction affords CF_3COO^- and that with $SbCl_5$ (in CH_2Cl_2) should furnish $SbCl_6$. Thus in particular CF_3COO^- seems to be solvated by CH_2Cl_2 in a much more efficient way than by, *e.g.* HFP, a rather astonishing observation.[29]

The simulations of the EPR spectra in the domain where the type ***A*** EPR spectra transform into the type ***B*** could not be accomplished by taking into account a two-jump process. However fairly closely matching simulations were possible by using a superposition of the two spectral types (Fig. 3). Using the ratios between the two types ***A*** and ***B*** and regarding the temperature, an activation barrier of 39 ± 10 kJ mol^{-1} can be estimated.

Optical spectra

The electronic absorption spectra obtained by SEOS spectroscopy indicate different absorptions when type ***A*** or ***B*** EPR spectra are detected. As expected, bands in the visible region start to emerge upon oxidation of **1**. The optical spectrum recorded simultaneously with the type ***B*** EPR signals (Fig. 2) closely resembles that obtained after reduction of **1** by electrolysis in DMF (counterion, $(Bu)_4N^+$)[28] hinting at the fact that the prominent absorptions stem from transitions between the singly occupied and adjacent orbitals in both radical ions. This similarity mirrors the pairing principle of orbitals in alternant hydrocarbons. The long-wave bands which emerge with the formation of the radical cation are at 535, 578, 636, 684 (sh) and 744 nm. The spectra connected with the delocalised species (***A***) display a much worse resolution and only weak bands at 539 and 746 nm are visible. Thus likewise on the time scale of the electronic transitions a distinction between the tight and loose ion pairs of $\mathbf{1}^{\bullet+}$ is possible.

Calculations

Using density functional theory, we have computed the counterion-free geometry of $\mathbf{1}^{\bullet+}$ (Fig. 5). Neutral **1** has a geometry in which the two anthracene moieties adopt a perpendicular orientation due to the steric hindrance by the protons in the 1,1′ and 8,8′ positions.[30] A UB3LYP/6-31G* calculation of $\mathbf{1}^{\bullet+}$ reveals an angle θ of 74°, *i.e.* an increased coplanarity of the two π systems (Fig. 5). Consequently, the ^1H

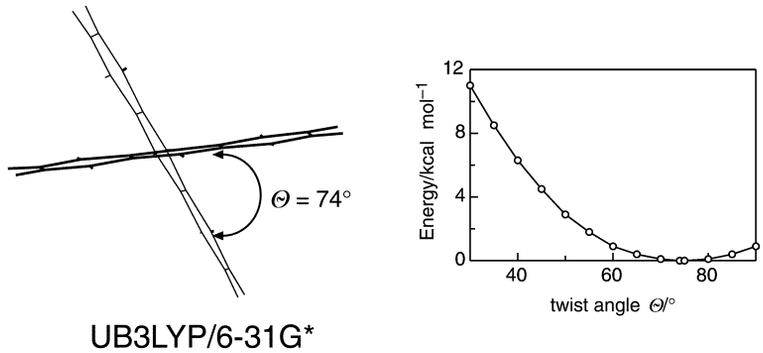

Fig. 5 Calculated geometries of counterion-free $\mathbf{1}^{\bullet+}$ and rotation barrier around the C(9)–C(9′) bond.

hfcs based on this geometry represent the delocalised form of $\mathbf{1}^{\bullet+}$ (***A***, Table 2). To check how flexible the connection between the two anthracene moieties is, we have computed the rotation barrier of $\mathbf{1}^{\bullet+}$ along the C(9)–C(9′) bond. The twist angle θ was fixed at the desired value and the molecule was optimised with this restriction. The rotation profile shown in Fig. 5 reveals that conformations with θ between *ca.* 60° and 90° are likely to be populated at the temperatures where the experiments were performed (*ca.* 273 K). At none of these geometries, however, did the calculations indicate the localisation of the spin and the charge; this is not unexpected since density functional theory calculations tend to overestimate electron delocalisation.[31]

According to these findings, the localisation of the charge and spin at one anthracene is exclusively due to the association with the counter anion. Trial calculations of $\mathbf{1}^{\bullet+}$ with a counterion led to ^{1}H hfcs of the bianthryl radical cation being far off the experimental values.

Conclusion

For the first time a clear-cut ion pairing effect has been established on localisation–delocalisation phenomena in radical cations of organic molecules. This states a structural alternative to former cyclovoltammetric measurements which anticipated that there is virtually no interaction between the two anthracene moieties in **1**, *i.e.* only "localised" species should exist: four successive and distinct oxidations of **1** are possible, leading to the radical cation, dication, (radical) trication and tetracation (solvent, SO_2; counterion, PF_6^-).[32] The potentials for the formation of the mono- and dication are rather similar (1.27 and 1.48 V *vs.* Ag/AgCl, respectively) and appear at almost the same voltage which has to be applied to obtain the anthracene radical cation (1.30 V *vs.* Ag/AgCl). This is even accentuated by the finding that the two further oxidation steps at 2.17 and 2.35 V *vs.* Ag/AgCl, close to the anthracene dication (2.10 V *vs.* Ag/AgCl) represent the formation of the tri- and tetracation. The geometry predicted by density functional calculations with a torsion angle θ of *ca.* 74° somehow resembles that postulated for the first excited singlet (S_1) state of **1** (θ *ca.* 62°).[33] This is a sensible analogy because the S_1 state is likely to possess similar properties as the corresponding radical cation.

For ion pairs between radical anions and (alkali) metal cations often additional splittings by magnetic metal nuclei establish the presence of tight ion pairs. Unfortunately such direct evidence by the occurrence of specific hfcs by magnetic nuclei present in the counter anions could not be established. Even the preference of certain counter anions for ion pairing is not straightforward.

Another assumption is that ion pairing may induce a more coplanar arrangement of the two anthracene moieties upon oxidation; *i.e.* tight ion pairs of $\mathbf{1}^{\bullet+}$ could possess a different molecular arrangement than the loose ones. However, it has to be borne in mind that very extended calculations have to be performed to shed only a diffuse light onto this aspect since such specific solute–solvent–counterion interactions are not likely to be correctly predicted by simple solvent models.

Association phenomena play an important role in numerous processes involving aggregation reactions, redox-coupled molecular magnets or electron transfer. This ranges from synthetic applications over material science to DNA chemistry. In this respect, an enhanced knowledge about the environmental effects onto the properties of radical cations seems valuable.

Acknowledgements

This contribution is dedicated to the late Lennart Eberson. I do not only want to acknowledge Lennart's significant contributions to the society of chemists but particularly appreciate his substantial benefit to my own research.

We thank the Swiss National Science Foundation for financial support.

References

1 M. Szwarc, *Ions and Ion Pairs in Organic Reactions*, Wiley, New York, London, Sydney, Toronto, 1972.
2 M. Scholz, G. Gescheidt and J. Daub, *J. Chem. Soc., Chem. Commun.*, 1995, 803.
3 M. Scholz, G. Gescheidt, U. Schoeberl and J. Daub, *J. Chem. Soc., Perkin Trans. 2*, 1995, 209.
4 M. Scholz and G. Gescheidt, *J. Chem. Soc., Perkin Trans. 2*, 1994, 735.
5 K. Exner, O. Cullmann, M. Voegtle, H. Prinzbach, B. Grossmann, J. Heinze, L. Liesum, R. Bachmann, A. Schweiger and G. Gescheidt, *J. Am. Chem. Soc.*, 2000, **122**, 10650.
6 H. Bock and U. Lechner-Knoblauch, *J. Organomet. Chem.*, 1985, **294**, 295.
7 W. Lau and J. K. Kochi, *J. Am. Chem. Soc.*, 1986, **108**, 6720.
8 W. Schmidt and E. Steckhan, *Chem. Ber.*, 1980, **113**, 577.
9 A. G. Davies and K. M. Ng, *Aust. J. Chem*, 1995, **48**, 167.
10 R. Erickson, N. P. Benetis, A. Lund and M. Lindgren, *J. Phys. Chem. A*, 1997, **101**, 2390.
11 J. V. Folgado, H. Garcia, V. Marti and M. Espla, *Tetrahedron*, 1997, **53**, 4947.
12 V. J. Rao, N. Prevost, V. Ramamurthy, M. Kojima and L. J. Johnston, *Chem. Commun.*, 1997, 2209.
13 T. Shida, E. Hasselbach and T. Bally, *Acc. Chem. Res.*, 1984, **17**, 180.
14 F. Bell and D. H. Waring, *J. Chem. Soc.*, 1949, 267.
15 G. Gescheidt, *Rev. Sci. Instrum*, 1994, **65**, 2145.
16 D. R. Duling, *PEST Winsim* (NIEHS, Research Triangle Park, NC, USA, 1995).
17 M. J. Frisch, G. W. Trucks, H. B. Schlegel, P. M. W. Gill, B. G. Johnson, M. A. Robb, J. R. Cheeseman, T. Keith, G. A. Petersson, J. A. Montgomery, K. Raghavachari, M. A. Al-Laham, V. G. Zakrzewski, J. V. Ortiz, J. B. Foresman, C. Y. Peng, P. Y. Ayala, W. Chen, M. W. Wong, J. L. Andres, E. S. Replogle, R. Gomperts, R. L. Martin, D. J. Fox, J. S. Binkley, D. J. Defrees, J. Baker, J. P. Stewart, M. Head-Gordon, C. Gonzalez, J. A. Pople, Gaussian 94, Revision B.3, Gaussian, Inc., Pittsburgh, PA, 1995.
18 A. D. Becke, *Phys. Rev. A*, 1988, **38**, 3098.
19 C. Lee, W. Yang and R. G. Parr, *Phys. Rev B*, 1988, **37**, 785.
20 U. Mueller and M. Baumgarten, *J. Am. Chem. Soc.*, 1995, **117**, 5840.
21 J. K. Kochi, R. Rathore and P. Le Maguères, *J. Org. Chem.*, 2000, **65**, 6826.

22 P. Le Maguères, S. V. Lindeman and J. K. Kochi, *Org. Lett.*, 2000, **2**, 3567.
23 O. W. Howarth and G. A. Fraenkel, *J. Am. Chem. Soc.*, 1966, **88**, 4514.
24 O. Hammerich and V. D. Parker, *Adv. Phys. Org. Chem.*, 1994, **20**, 1.
25 A. J. Bard, A. Ledwith and H. J. Shine, *Adv. Phys. Org. Chem.*, 1976, **12**, 155.
26 O. W. Howarth and G. A. Fraenkel, *J. Chem. Phys.*, 1970, **52**, 1573.
27 F. Gerson, G. Kaupp and H. Ohya-Nishiguchi, *Angew. Chem.*, 1977, **89**, 666.
28 G. Grampp, A. Kapturkiewicz and J. Salbeck, *Chem. Phys.*, 1994, **187**, 391.
29 L. Eberson, M. P. Hartshorn and O. Persson, *J. Chem. Soc., Perkin Trans. 2*, 1995, 1735.
30 H. D. Becker, V. Langer, J. Sieler and H. C. Becker, *J. Org. Chem*, 1992, **57**, 1883.
31 T. Bally and G. N. Sastry, *J. Phys. Chem. A*, 1997, **101**, 7923.
32 M. Dietrich, J. Mortensen and J. Heinze, *Angew. Chem.*, 1985, **97**, 502.
33 J. J. Piet, W. Schuddeboom, B. R. Wegewijs, F. C. Grozema and J. M. Warman, *J. Am. Chem. Soc.*, 2001, **123**, 5337.